A Robust Approach to Depth of Anaesthesia Assessment Based on Hybrid Transform and Statistical Features

Mohammed Diykh[1,2✉], Firas Sabar Miften[2], Shahab Abdulla[3], Khalid Saleh[5], and Jonathan H. Green[3,4]

[1]School of Agricultural, Computational and Environmental Sciences, University of Southern Queensland, Australia

[2]University of Thi-Qar, College of Education for Pure Science, Iraq

[3]Open Access College, University of Southern Queensland, Australia

[4]Faculty of the Humanities, University of the Free State, South Africa

[5]School of Mechanical and Electrical Engineering, University of Southern Queensland, Australia

✉First and corresponding author: Mohammed Diykh, School of Agricultural, Computational and Environmental Sciences, University of Southern Queensland, Australia.

E-mail: mohammed.diykh@usq.edu.au

Abstract: To develop an accurate and efficient depth of anaesthesia (DoA) assessment technique that could help anaesthesiologists to trace the patient's anaesthetic state during surgery, a new automated DoA approach was proposed. It applied Wavelet-Fourier analysis (WFA) to extract the statistical characteristics from an anaesthetic EEG signal and to designed a new DoA index. In this proposed method, firstly, the wavelet transform was applied to a denoised EEG signal, and a Fast Fourier transform was then applied to the wavelet detail coefficient D3. Ten statistical features were extracted and analysed, and from these, five features were selected for designing a new index for the DoA assessment. Finally, a new DoA (WFA_{DoA}) was developed and compared with the most popular Bispectral index (BIS) monitor. The results from the testing set showed that there were very high correlations between the WFA_{DoA} and the BIS index during the awake, light and deep anaesthetic stages. In the case of poor signal quality, the BIS index and the WFA_{DoA} were also tested, and the obtained results demonstrated that the WFA_{DoA} could indicate the DoA values, while the BIS failed to show valid outputs for those situations.
.

1. Introduction

Depth of anaesthesia (DoA) monitoring during surgical operation is a very challenging task [1-7]. An accurate assessment of the DoA helps correctly deliver anaesthesia agents to patients and prevent unintended intraoperative awareness [8-14]. After an anaesthetic agent is applied to a patient, the drug affects the central nervous system. The amplitude and frequency of EEGs change rapidly and are reflected the changes of the anaesthetic depth [15]. That is why EEG signals have been widely used as a powerful tool to capture the information about anaesthetic depth. As a result, many techniques for DoA estimation have been developed based on EEG signals[16-20].

Among the many DoA monitoring devices, the Bispectral index (BIS), developed in 1992 by Aspect Medical Systems [21,22], is the most popular. The BIS index was designed using a set of parameters that were derived from different transformation techniques, such as the techniques from time domain and frequency domain [23-26]. Monitoring the depth of anaesthesia accurately can prevent intraoperative awareness and overdose. In the past two decades, the BIS has been widely used for monitoring the DoA. At the same time, many other devices and techniques have been developed. For example, Lalitha and Eswaran [1], used non-linear features and two neural network classifiers were applied to identify

the DoA. A correction dimension, a Lyapunov exponent and a Hurst exponent were extracted as the key features from the EEG data. The extracted features were forwarded to two neural networks: a multi-layer perceptron and an Elman network, for assessing the DoA. Additionally, Nicolaou *et al*. [27], developed a method for distinguishing two states of awake and anaesthetized. In their study, the EEG recordings were segmented, and two states: loss consciousness at induction and recovery consciousness after ending surgery were identified. A Granger causality method was developed to extract the features from each sequential EEG segment. A linear discrimination and a support vector machine were used in the classification phase. Esmaeili *et al*. [9], on the other hand, developed a fuzzy model to identify the anaesthetic depth. In their study, a single EEG channel was analysed in the time and frequency domains. The spectrum characteristics, such as alpha-ratio, beta ratio and theta-ratio were extracted and those features were then analysed and tested using a statistical approach to design a cost function for a fuzzy classifier.

Moca *et al*. [21], proposed an automatic method for assessing the DoA based on a multi-feature extraction. A time encoded signal processing and recognition (TESPAR) method was used to detect the DoA. In their study, an EEG signal was split into segments based on zero crossing. The TESPAR was

1

employed to capture the information that was difficult to obtain in frequency domain. The extracted characteristics were used as the input to a multi-layer perceptron. Nguyen-Ky *et al*.[27], measured the DoA using a wavelet transform. The EEG signal was decomposed into different levels to extract the desired frequencies. As a result, six bands: θ-band, α-band, β-band, δ-band, γ-band and EMG, were extracted, and then an eigenvector of wavelet coefficients were calculated. An index was designed based on the statistical characteristics of the extracted features and was compared with the BIS index. Staikou *et al*.[36], investigated the impact of intravenous lidocaine on the DoA. A total of 78 subjects were involved in that study. The BIS was used to monitor the DoA. The results showed that giving intravenous lidocaine during rapid sequence induction did not affect the BIS values. Shepherd *et al*.[33], made a study to assess the clinical effectiveness and cost-effectiveness of BIS, E-Entropy and Narcotrend by comparing each one with standard clinical monitoring, to monitor the DoA in surgical patients undergoing the general anaesthesia. Tiren *et al*. [38], made a clinical study in which the BIS and Entropy monitoring were compared in patients undergoing heart surgery. Their results showed that the BIS indicated deep anaesthesia more accurately than entropy. Bankman and Gath [3], applied fuzzy logic for the DoA assessment. They applied an adaptive segmentation technique to extract nine time frequency features from each EEG segment, then a sequential fuzzy clustering algorithm was utilized to classify the extracted features into one of the anaesthetic states. Shalbaf *et al*.[31], assessed the depth of anaesthesia using EEG signals. A permutation entropy and a sample entropy were extracted from the denoised EEG signals, and the features then were fed to an artificial neural network. The research yielded an accuracy of 92.4%.

More recently, Shalbaf *et al*. [32], also has proposed a method for the DoA identification based on a modified permutation entropy. The features were extracted from each 10-s EEG segment. All the features were then fed to a linear discrimination analysis structure to distinguish different anaesthetic states. Shi *et al*. [34], proposed a predictive model for the depth of anaesthesia assessment based on local field potentials (LFPs). The LFPs were decomposed into six consecutive components using a wavelet transform. The high frequency features were selected and a Lempel-Ziv Complexity was calculated from LFPs. In the literature, much effort has been expended in extracting features from EEG signals and in designing DoA indexes using different methods, such as neural networks, fuzzy systems, a support vector machine, *etc*.[34,35]. Most of the feature extraction methods were related to using a Fourier transform or a Wavelet transform to pull out the key characteristics of EEG signals [36-38]. Those techniques mainly aim to reduce the dimensionality of the EEG data and increase the accuracy of the DoA estimation.

In this paper, the wavelet transform was utilized to decompose the denoised EEG signals. The number of the decomposition levels was empirically determined. As a result, the wavelet detail coefficient D3 was chosen for further processing using a fast Fourier transform. Then ten statistical features were extracted to develop a new DoA index (WFA_{DoA}). Finally, the WFA_{DoA} was assessed and compared with the recorded BIS index.

2. Material and Method

2.1 EEG data

Ethical approval was obtained from the Human Research Ethics Committee of University of Southern Queensland (No: H09REA029) as well as from Darling Downs Health Service District Human Research Ethics Committee (No: TDDHSD HREC 2009/016), Australia. The data were collected by the attending anaesthetist who documented the time, intravenous dosing and significant intraoperative events. All the participants signed on the consent forms in advance. A total of 37 adult patients, 15 females and 22 males, were involved. Subjects were aged from 22-83 years old, weighed between 55-130 kg, and averaged at 174 cm in height. The recommended drug administration consisted of midazolam 0.05 mg/kg, fentanyl 1.5-3 µg/kg or alfentanil 15-30 µg/kg. The EEG data were recorded using four adhesive forehead Quatro electrodes sensors, and were stored in a desktop computer for off-line processing. The data file obtained included the real time log, EEG data, the BIS index and the monitor log of errors. The EEG signals were acquired from two channels: channel-1 and channel-2. The EEG data from channel-2 were selected, as the simulation results showed that the frequency characteristics of EEG signals from Channel-2 were more highly correlated to aesthetic states than those from channel-1. The EEG signals from channel-2 were sampled at a frequency of 128, and each EEG sample was a 16-bit signed integer.

2.2 Signal denoising and pre-processing

Due to contamination from different types of noise, such as muscle artefacts and ECG, *etc*, the EEG signals could not be used directly without a denoising technique A nonlocal mean method was used to denoise the collected EEG data. The details of the denoising process were introduced in Li *et al*.[17].

Data with signal quality index (SQI) values of more than 15 were selected in this study. As a result, subjects 2-5, 7, 8, 11, 12, 13, 18, 19, 20, 24, 25, 29 and 30 were chosen. The remaining subjects were also chosen for the purpose of assessing the ability of the proposed DoA index to estimate the DoA in the case of poor signal quality. The selected subjects were divided into two sets. One set was used for selecting the optimum parameters and designing the proposed index while the second set was used for testing the proposed index.

2

3. Methodology

The proposed Wavelet-Fourier analysis method started with EEG signal segmentation using a moving window technique. The window size was 56 s with an overlap of 55 s. The statistical features of the EEG signal were then extracted. Based on the results, it was found that statistical features extracted from EEG signals using the WFA performs were better than the others in showing changes in EEG signals during the DoA. As a result, the five features (standard deviation, entropy, median, root mean square, min) obtained using the WFA were selected. Finally, the WFA_{DoA} was designed using these statistical features. Figure 1 describes the methodology of the DoA.
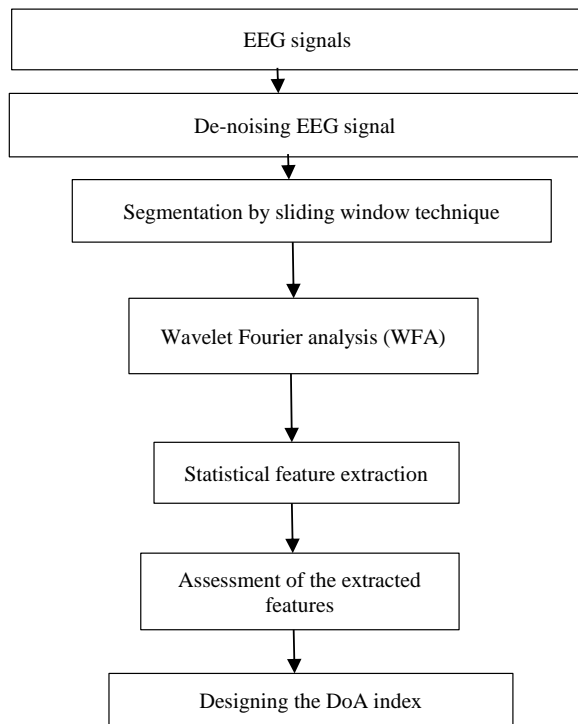
EEG signals

De-noising EEG signal

Segmentation by sliding window technique

Wavelet Fourier analysis (WFA)

Statistical feature extraction

Assessment of the extracted features

Designing the DoA index

Fig. 1. Methodology of DoA identification

3.1 Discrete wavelet transform

The discrete Wavelet transform (DWT) was employed for decomposing the EEG signals. The DWT of an EEG signal x was defined [24] as

$$DWT(i,j) = \frac{1}{\sqrt{|2^i|}} \int_{\infty}^{\infty} x(f)\psi\left(\frac{t-2^i k}{2^i}\right) \qquad (1)$$

where $DWT(i,j)$ was wavelet coefficients, $x(f)$ was the EEG signal, $\psi(.)$ was a wavelet function, and 2^i and k were scaling factors.

The DWT decomposes a signal into different frequency bands. As a result, a set of approximation and details were obtained after transforming the EEG signal through a sequence of high and low pass filters.

Figure 2 shows a signal that is decomposed into a set of approximations and details. Two digital filters and two down-sampled outputs are involved at each decomposition level. At the first level, the high pass and low pass filters are produced as the detail (D1) and the approximation (A1). For further decomposition, the same process can be performed for the approximation A1. This process is continuously repeated to obtain a desired output. To choose an appropriate number of the decomposition level and a type of wavelet, different wavelets were tested in this paper. It was found that the Daubechies (db6) produces more acceptable results than other wavelet functions. The six sub-bands were D1, D2, D3, D4, D5 and A5. A5 is the decomposition approximation coefficients and D1-D5 are the decomposition detail coefficients. It was observed that the six-level wavelet decomposition and Daubechies (db6) yielded better results compared to others. Therefore, in this study D3 was chosen empirically.

3.2 Discrete wavelet transform

FFT is a fast method to compute the discrete Fourier transform (DFT). Let $x(k)$ refer to a continuous signal. The Fourier transform of signal $x(k)$ would be described as

$$X(ju) = \sum_{\infty}^{\infty} x(k)e^{-jut} \qquad u \in (-\infty, \infty) \qquad (2)$$

The transform pair of the DFT is defined as

$$X(k) = \sum_{n=0}^{N-1} h_k e^{j\frac{2\pi}{N}nk} \qquad (3)$$

where $h_k = \frac{1}{N}\sum_{m=0}^{N} x(k)e^{-j\frac{2\pi}{N}nk}$.

For a periodic signal with N samples, the DFT can be depicted as the discrete time Fourier transform.

$$x = \begin{bmatrix} x(0) \\ x(1) \\ . \\ . \\ x(N-1) \end{bmatrix}, \qquad X = \begin{bmatrix} X(0) \\ X(1) \\ . \\ . \\ X(N-1) \end{bmatrix} \qquad (4)$$

$$W = [W_N^{kn}] = \begin{bmatrix} 1 & 1 & . & . & . & 1 \\ & W_N & & & & \\ . & . & & & & \\ 1 & W_N^{N-1} & . & . & W_N^{(N-1)(N-1)} \end{bmatrix} \qquad (5)$$

The relationship between x and X is described as

$$X = W_x \leftrightarrow x = \frac{1}{N}W^{H_x} \qquad (6)$$

3.3 Wavelet Fourier analysis

The wavelet decomposition was used as a classifier in this study, while the FFT was applied to visualize EEG waves to obtain more effective features. In each decomposition stage of the DWT, the number of multiplications is divided by two due to a down-sampling operation, but wavelet coefficients for each level still contain the full information. If the DFT is applied to the wavelet coefficients, the frequency information

3

about the signals can be obtained with a few required multiplications [40, 41].

The DWT was applied to the EEG signal as the first step for decomposing an EEG signal into different scales and for obtaining the wavelet detail coefficients and the approximation coefficients. Then, the FFT was applied to each level of the DWT to determine the best level of decompositions. As a result, it was found that D3 provides specific and individual frequency characteristics for each

statistical features were mean, entropy, standard deviation, root mean square, variation, mode, skewness, Kurtosis, range, and minimum, denoted respectively as X_{Min}, $X_{entropy}$, X_{Mean}, X_{SD}, X_{RMS}, X_{Var}, X_{Ske}, X_{Rang}, X_{Mod}, X_{Ku}. A regression technique and Pearson correlation were used to test the relationships between the features and the anaesthetic
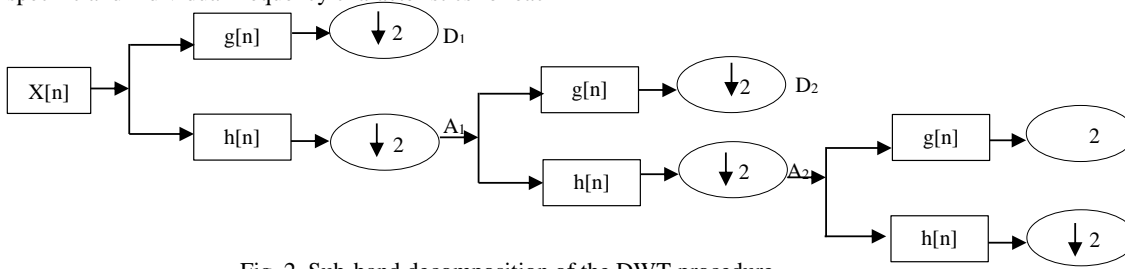

Fig. 2. Sub-band decomposition of the DWT procedure

state of the DoA. The combination of the DWT and the FFT was used to extract the final statistical features vector. The following algorithm was used to obtain the optimum wavelet decomposition level for further processing using Fourier transform.

Input   *X= EEG signals*
Algorithm

1. *Let p be a number that EEG signals should be decomposed, initially K=0*
2. *For each EEG segment do*
3. *K=K+1*
4. *Decompose EEG signals into K level using DWT*
5. *passing the outputs of step 4 to FFT*
6. *extracting the statistical features*
7. *Evaluate the extracted features to design DoA*
8. *if the extracted features correlated with the BIS then stop decomposing, go to step 10*
9.   *else go to step 3*
10. *end*

Output   a set of statistical features and decomposition level (P)

Ten statistical features were extracted from each EEG segment after applying the DWT, FFT and WFT. Based on the results, it was found that it was difficult to recognize the DoA with the selected statistical features using the DWT and the FFT separately. However, it was observed that when the WFA was utilized to extract the selected features, the states of the DoA could be better identified.

Table 1 provides a short explanation of the statistical features used in this work. The statistical features were extracted after applying the WFA to the EEG signals. Ten of them were calculated and tested to assess each feature and to determine the best combinations for the WFA_{DoA} development. The 10

states. The absolute values of statistical features were considered in our paper. Based on the results obtained, the standard deviation, min and entropy from β band and the median and root mean square from θ band were selected as the key features to represent the original EEG signals.

We noticed that the increasing and decreasing of the BIS values corresponded to the changing in the values of the selected features, and vice versa.

3.4 Features extraction

The ten features (X_{Min}, $X_{entropy}$, X_{Mean}, X_{SD}, X_{RMS}, X_{Var}, X_{Ske}, X_{Rang}, X_{Mod}, X_{Ku}) were extracted from each of the five bands (δ, θ, α, β, γ). Total (5 x N) feature vectors were obtained from the original EEG signal, where 5 is the number of bands and N represents the number of EEG segments. Each feature vector was tested to evaluate the correlations with the BIS index. All the features were evaluated using the coefficients of determination, R2, which is a statistical test to examine how close the data are fitting the regression line. It is defined by the following formula.

$$R^2 = 1 - \frac{\sum_i (y_i - f_i)^2}{\sum_i (y_i - \bar{y})^2} \qquad (7)$$

where, y_i is the BIS value, f_i is the estimated value (in this paper it refers to the statistical features) and $\bar{y}$ is the mean of y_i. The R2 value ranges from 0 to 1. A higher R2 value refers to the higher correlation between the extracted features and the anaesthetic states, and vice versa. Based on Table 2, the set of features of (standard deviation, entropy, median, root mean square, min) was selected to represent the original EEG data. The selected features were further tested using a scatter plot graph. Figures 3-7 show an example of the scatter plot graphs of the selected features for subject No.7. The same procedure was repeated for all the subjects to select the optimum features.

4

The linear relationships between the features and the BIS values in Figures 3, 4, 5, 6 and 7 indicate that the features are correlated with the BIS. We can notice that the entropy linear equation fits to all the data with a relation of BIS=0.0214x+3.246. For RMS, min, median and standard deviation, the linear equation is fitted to all the data with a relation as 0.0167x+3.2236, 0.6235x+15.606, 0.0193x+3.3403 and 0.8559x+3.9501 respectively.

$$T2 = \sum_{1}^{n}(0.6235 \times min + 15.606) + (0.167 \times RMS + 15.606)$$
$$+ (0.8559 \times standard\ deviation + 3.9501)$$

The formula of the WFA_{DoA} was finalized after several experiments were conducted and tested with all the subjects. We found that some of WFA_{DoA} values are beyond the BIS index range. To resolve this issue a normalization technique was used. WFA_{DoA} was normalized as follows:

Table 1

Short clarification of statistical features

No.	Feature name	Formula	No.	Feature name	Formula
1	Mean	$X_{Mean} = \frac{1}{n}\sum_{1}^{n} x_i$	6	Minimum	$X_{Min}=\min[x_n]$
2	Entropy	$X_{entropy} = -\sum_{i=1}^{m} p(X_i).log_2 p(x_j)$	7	Mode	$X_{Mod} = L + \left(\frac{f_1 - f_0}{2f_1 - f_2}\right)Xh$
3	Standard deviation	$X_{SD} = \sqrt{\sum_{n=1}^{N}(x_n - AM)\frac{2}{n-1}}$	8	Range	$X_{Rang} = X_{max} - X_{min}$
4	Root mean square	$X_{RMS} = \sqrt{\frac{\sum_{i=1}^{m} x_i^2}{m}}$	9	Skewness	$X_{Ske} = \sum_{n=1}^{N}(x_n - AM)\frac{3}{(N-1)SD^3}$
5	Variation	$X_{Var} = \sum_{n=1}^{N}(x_n - AM)\frac{2}{N-1}$	10	Kurtosis	$X_{Ku} = \sum_{n=1}^{N}(x_n - AM)\frac{4}{(N-1)SD^4}$

Table 2

The highest R^2 value of the statistical feature in five bands

Features/Band	δ	θ	α	β	γ
Range	0.014	0.064	0.0010	0.0021	0.0011
Standard deviation	0.0113	0.253	0.021	**0.2121**	0.102
Min	0.124	0.174	0.042	**0.297**	0.111
Median	0.101	**0.397**	0.130	0.121	0.061
Mode	0.120	0.015	0.120	0.141	0.213
Entropy	0.012	0.272	0.110	**0.4206**	0.012
Variation	0.012	0.036	0.098	0.087	0.059
skewness	0.0101	0.0011	0.108	0.0301	0.013
Kurtosis	0.0041	0.0021	0.008	0.019	0.064
Root mean square	0.0010	**0.3523**	0.0107	0.0021	0.001

As a result, the features (RMS, entropy, standard deviation, median, minimum) were selected. Considering the relationships with the BIS, we designed the WFA_{DoA} for assessing the DoA as below:

$$WFT_{DoA} = \frac{T1 + T2}{F} \qquad (8)$$

where F is a threshold (empirically determined), and T1 and T2 defined as:

$$T1 = \sum_{1}^{n}(0.014 \times entropy + 3.246) + (0.193 \times median + 3.3403)$$

$$If\ WFA_{DoA} > 100 \rightarrow WFA_{DoA} = 100 \qquad (9)$$
$$If\ WFA_{DoA} < 0 \rightarrow WFA_{DoA} = 0 \qquad (10)$$

4.1 Agreement of the new Index and BIS Index

The Bland-Altman was employed to measure the main differences and estimate the agreement between the BIS and WFA_{DoA}. Firstly, we defined the differences between the BIS and the WFA_{DoA} as diff = $(WFA_{DoA} - BIS)$, and then the mean and the standard deviation of diff were calculated as Mdif=mean (diff), Stdif=std (diff). The Bland-Altman

5

Auto-generated PDF by ReView
This article has been accepted for publication in a future issue of this journal, but has not been fully edited. Content may change prior to final publication in an issue of the journal. To cite the paper please use the doi provided on the Digital Library page.
IET Science, Measurement & Technology

suggested that 95% of data points should lie within (Stdif - Mdif) of the main difference[9]. The main differences were calculated and plotted in Fig. 8. Figure 9 shows the normal distribution of the differences between the BIS and the WFA_{DoA} for two subjects (No.7 and No.11). From Figs. 8 and 9, the normal fit matches well with the distribution differences.

Root mean square (RMS)

y = 0.0167x + 3.2236
R² = 0.3523

Fig.5 Scatter graph of *RMS* and the BIS

Standard deviation

y = 0.8559x - 3.9501
R² = 0.21

Fig.3 Scatter graph of *standard deviation* and the BIS

Min

y = 0.4325x + 23.474
R² = 0.297
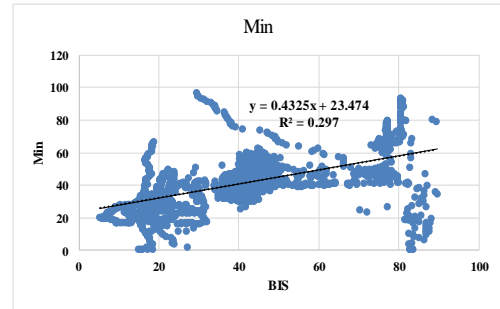
Fig.6 Scatter graph of *min* and the BIS

Median

y = 0.0193x + 3.3403
R² = 0.397

Fig.4 Scatter graph of *median* and the BIS

Entropy

y = 0.0214x + 3.246
R² = 0.420
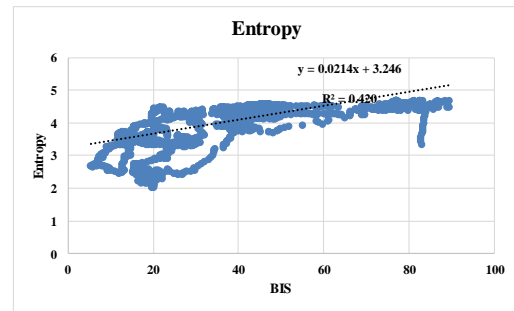
Fig.7 Scatter graph of *Entropy* and the BIS

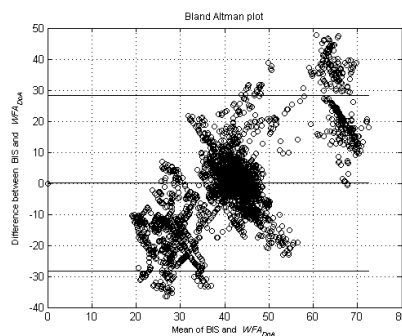Bland Altman plot

Bland Altman plot
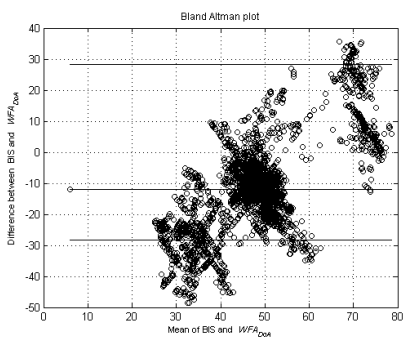
Fig. 8. Bland Altman plot of WFA_{DoA} and the BIS

6
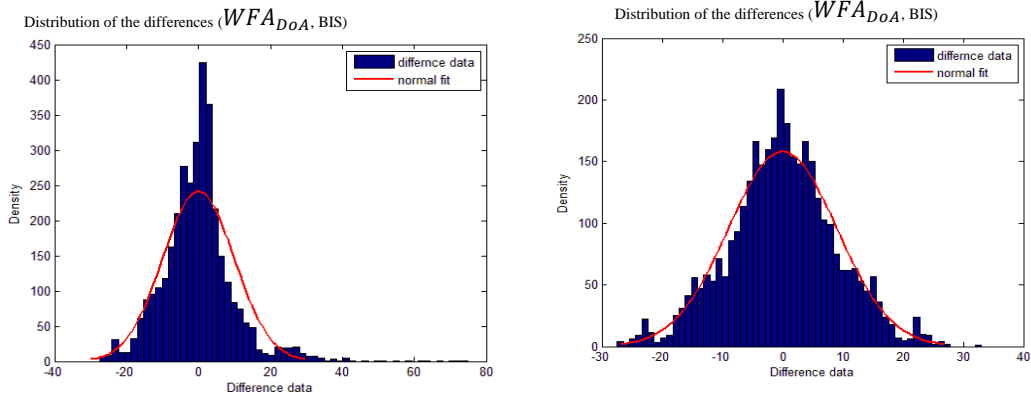
Fig. 9. The normal distribution plot of WFA_{DoA} and the BIS

a. Subject No. 2

c. Subject No. 12

b. Subject No. 18
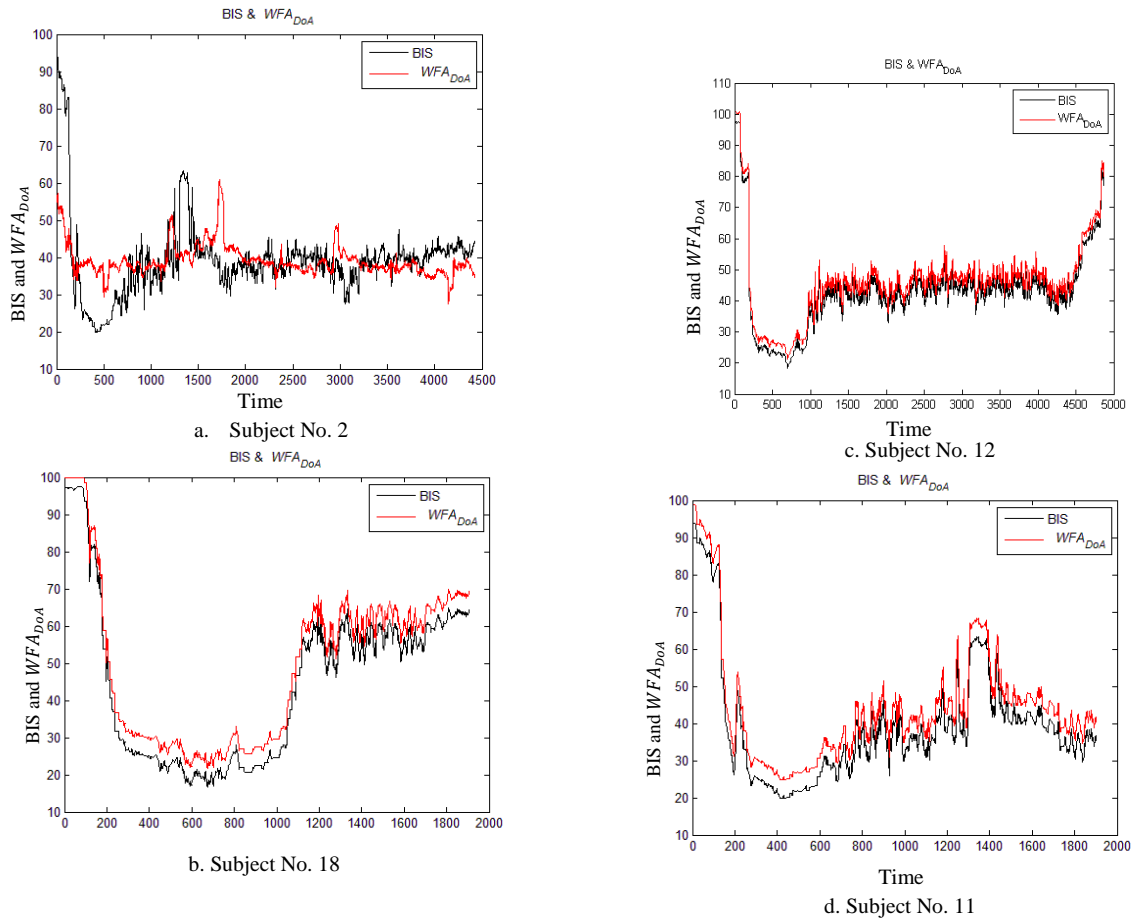
d. Subject No. 11

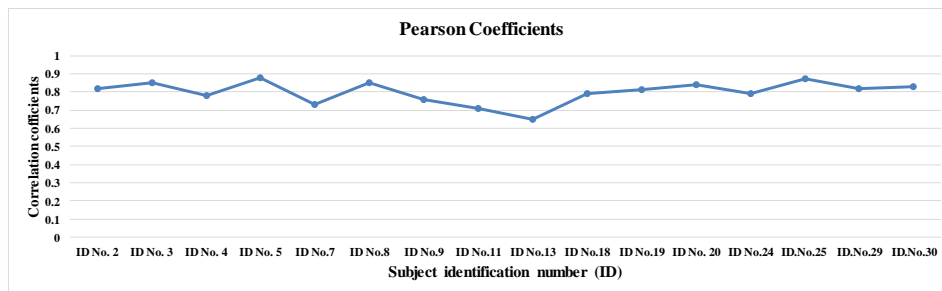Fig. 10. Comparison of performance between WFA_{DoA} and the BISf

Fig. 11. Pearson coefficients for all the subjects

7

4.2 Pearson Correlation

Further investigations were made to evaluate the ability of the proposed index to identify the depth of anaesthesia The Pearson correlation technique was also used to evaluate the relationships between the BIS and the WFA_{DoA}. It describes the strength of a linear relationship between two populations (in this work, the two populations are the BIS and the WFA_{DoA}). For example, if the two populations have a straight line relationship in the positive direction, the value of the correlation will be positive (> 0), If the linear relationship has negative value (<0), it means there is a negative relationship between the two samples. However, the zero value refers to the absence of relationships between the two populations.

The proposed method was implemented using the selected subjects and then the correlation method was applied to test the obtained results.

Fig. 10 shows examples of experiments from the 16 subjects. The obtained results from subjects Nos: 2, 11, 12 and 18 were chosen as the examples. It demonstrated that there are very high correlations between the WFA_{DoA} and the BIS during the awake, light and depth anaesthetic stages. When the BIS value goes up or drops down, the WFA_{DoA} values also change. The Pearson coefficients were also calculated between the BIS and the WFA_{DoA} for all the subjects. Figure 11 shows the Pearson correlation coefficients for the chosen subjects. It can be seen there is a very strong relationship between the WFA_{DoA} and the BIS values. This reflects the strong agreement between the WFA_{DoA} and the BIS. The average of correlation coefficients between the WFA_{DoA} and the BIS was 0.798 for the 16 subjects.

4. Discussion

In this paper, a new approach for depth of anaesthesia assessment was presented. The following four steps were considered to assess the DoA in this paper:

1. The EEG signals were filtered to obtain high quality denoised EEG signals. In this phase the nonlocal mean denoising method was used to remove artefacts such as Electromyographic (EMG) and electrocardiograms (ECG) from EEG signals. Because if any ECG and EMG are not removed from EEG signals then EEG epochs are considered unusable in the index designing, and also, the Signal Quality Indicator (SQI) is decreased. The NLM was applied to simulated EEG signals with Gaussian white noise, spiking noise and specific frequency noise before being applied to the real EEG signal from hospitals.

2. In the segmentation phase, different experiments were carried to choose the window size due to the window length was an important factor that could affect the performance of the proposed index and the efficiency of the extracted features. In this paper, a fixed length sliding window of 56s was adopted for reading and processing the EEG data. An overlapping of 55 s was adopted after different values of the window

overlapping were tested with ranging from 1s to the maximum value 55s.

3. A combination of wavelet Fourier transforms were utilized to analyse EEG signals so that the representative features could be extracted to design the DoA index. Our findings showed that when the discrete Wavelet transform and fast Fourier transform method were integrated and applied to EEG signals, the important characteristics of EEG signals were revealed.

4. A new index (V WFA_{DoA}) was designed after a thorough investigation was made to select the most powerful features. The developed index was tested and assessed using different statistical metrics and the results showed that the ability of the proposed index to trace the DoA efficiently. To determine whether the WFA_{DoA} has similar distribution shape and similar tail behavior as the BIS, the quantile-quantile plot (Q-Q plot), which is a graphical approach used to determine the validity of two methods, was used for further investigation. In Q-Q plot, a reference line is plotted. If the WFA_{DoA} and the BIS index have the same distribution, their points should fall approximately along this reference line. Fig.12 shows the Q-Q plot of the WFA_{DoA} and the BIS index for four subjects of ID Nos: 18, 11, 7 and 2. From the obtained results in Fig. 12, we can observe that the WFA_{DoA} and the BIS have a similar distribution.

The BIS monitor shows a signal quality index as well as a real time EEG signal, BIS values, EMG, and burst and suppression ratio [34-36]. The BIS index is considered an efficient method to trace the depth of anaesthesia. However, the main concern of using the BIS index is that it could fail to display the values on the screen and may not fully reflect the anaesthetic states when the signal quality is lower than 15. The signal quality of an EEG channel is measured by using a signal quality indicator (SQI) and it is calculated based on different variables, such as artefacts, impedance data etc. A higher SQI number (SQI>15) refers that the BIS values are reliable and more accurate while a lower SQI number (SQI<15) indicates that the BIS values could not be displayed on screen along with other variables and parameters. In this paper, the WFA_{DoA} was tested using the same poor quality signals. The results showed that the proposed index can generate and display the index values correctly. Fig. 13a shows the poor signal quality case for subjects Nos. 27 and 37. The information include the time and the medication type. For subject No. 27, as an example, the surgery started at 10:31:33 am, and continued to 10:52:26 am. From 100 to 400 seconds (10:31:33 am to 10:34:33am), the BIS could not show the DoA values. In this case the state of the subject cannot be estimated. In Fig 13b, we can also observe that the BIS also failed to display the DoA values from 200 to 500 seconds while the WFA_{DoA} was able to estimate the DoA. Table 3 provides the details of the drug administration for both subjects. For the sake of evaluation,

8

Table 3

Details of aesthesia medications for Subject 27 and 37

Subject Number	Drug	Time
Subject 27	Midazolam 4	10:31:35 am
	Alfentanil (100 ug)	10:31:55 am
	Parecoxib (40 mg)	10:32:55 am
	Propofol (160 mg)	10:33:30 am
	Desflurane and nitrous oxide	10:33:35 am
Subject 37	Midazolam 3	10:13:15 am
	Alfentanil (100 ug)	10:13:35 am
	Parecoxib 40	10:16:30 am
	Morphine 5	10:19:00 am
	Propofol 60	10:19:05 am
	Morphine 5	10:40:53 am

a.Q-Q plot of subject 7

b.Q-Q plot of subject 2

c.Q-Q plot of subject 11

d.Q-Q plot of subject 18
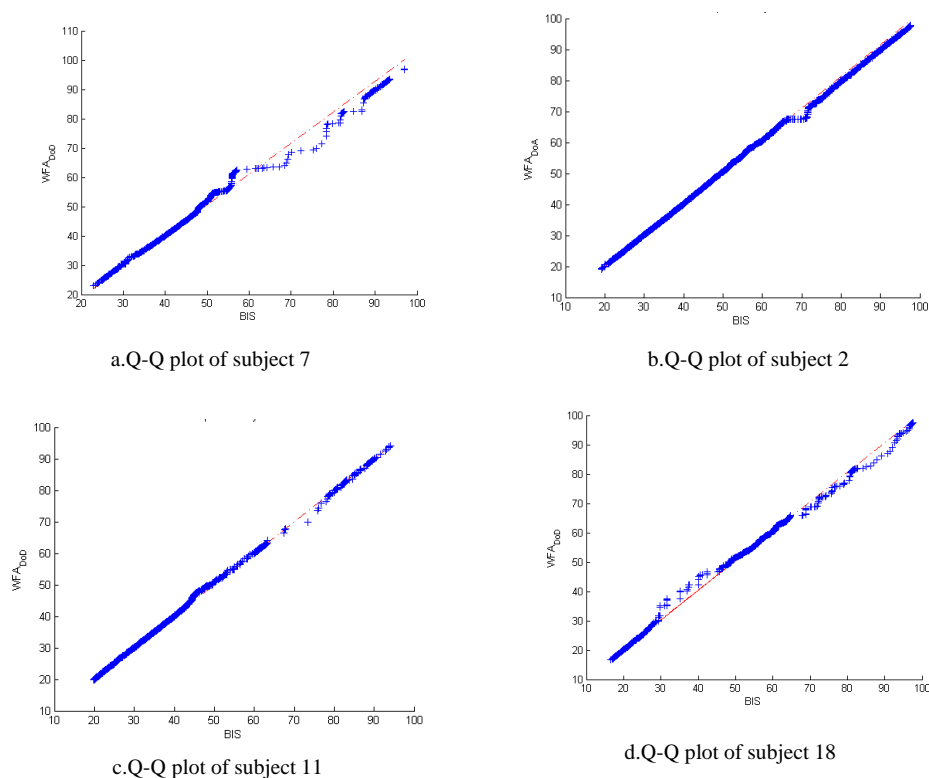
Fig. 12. Q-Q plot of subject 2, 7, 11 and 18

9

a. Subject No. 27
b. Subject No. 37
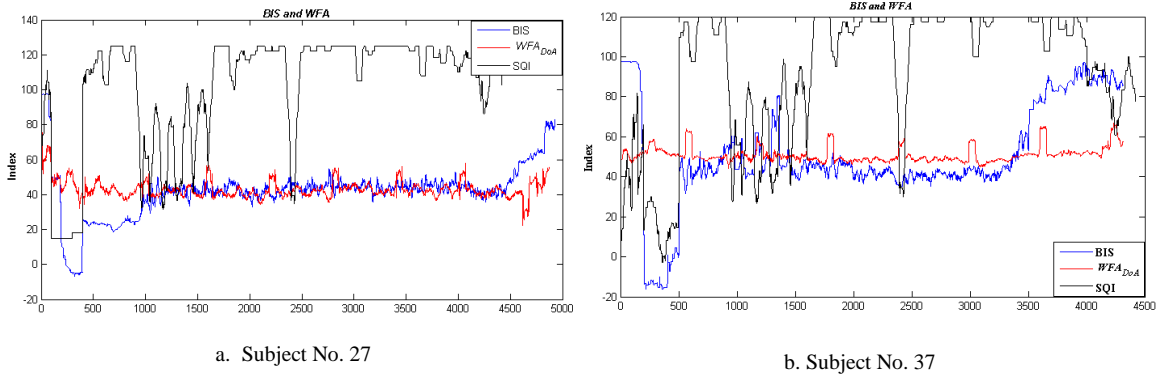
Fig. 13. Examples of poor signal quality cases (subjects No. 27 and No. 37)
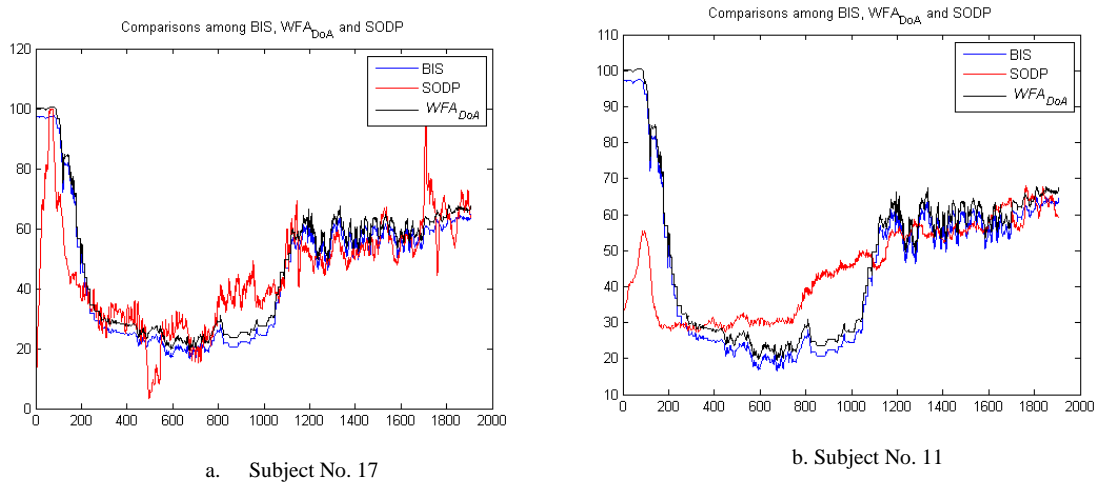

a. Subject No. 17
b. Subject No. 11

Fig. 14. Comparisons between the proposed index with DODP index

the proposed method was compared to a previous study which was developed by Li et al., 2016. All EEG recordings were used in this comparison. The characteristics of second order difference plot were considered to trace the DoA in that study. Li et al., 2016 used the same dataset as we did in our study to evaluate their proposed DoA index. Fig.14 shows comparisons between our proposed index with SODP against the BIS. From Fig.14 it can be observed that the proposed index has a high correlation with the BIS than the SDOP index during the anaesthetic states. The results showed our proposed index values rose or dropped when the BIS values changed, while the SDOP index did not produce highly correlated values with the BIS.

To choose the level of decomposition in wavelet transform, we investigated each level of decomposition by repeating the same procedures in sections 2.3.3, 2.3.4, 2.3.5 and section 3. It was found that there was a good relation between a patient clinical state and the extracted features with level 3

decomposition. The values of the features were high during the conscious state and lower during the unconscious states.
In this study, five features from ten extracted features were selected and used based on statistical analysis. The WFA_{DoA} was designed using those features. The results showed that the index can measure the DoA with a high accuracy compared with the BIS index. In future work, we will work to decrease the number of features used and to extend this method to other application areas, such as detecting seizures, sleep stages classification etc.

5.Conclusion
A robust approach for the DoA assessment based on the WFA and statistical features is proposed. In this method, ten statistical features were extracted from each EEG segment using the WFA. These features were then tested, and five features was selected based on their coefficients of determination as the key features to design the WFA_{DoA}. The WFA_{DoA} was then evaluated, and the results showed that the index can measure the DoA with a higher degree of accuracy than the BIS index. Furthermore, the WFA_{DoA} was also tested, and performed well and better than the BIS. In future, we will

10

work to decrease the number of features used and to extend this method to other application areas, such as detecting seizures, sleep stages classification, and other similar areas of application.

References

1. Arslan, A., Sen, B., Çelebi, F.V., Peker, M., and But, A., 'A Comparison of Different Classification Algorithms for Determining the Depth of Anesthesia Level on a New Set of Attributes', in, Innovations in Intelligent SysTems and Applications (INISTA), 2015 International Symposium on, (IEEE, 2015).

2. Ball, C. and Westhorpe, R., 'The History of Depth of Anaesthesia Monitoring', Anaesthesia and intensive care, 2010, 38, (5), pp. 797-798.

3. Bankman, I. and Gath, I., 'Feature Extraction and Clustering of Eeg During Anesthesia', Medical amd Biological and Computing, 1987. 25, (4), pp.474-477.

4. Bard, J.W., 'The Bis Monitor: A Review and Technology Assessment', AANA journal, 2001, 69, (6), pp. 477-484.

5. Bibian, S., Zikov, T., Dumont, G.A., Ries, C.R., and Puil, E., Estimation of the Anesthetic Depth Using Wavelet Analysis of Electroencephalogram', (DTIC Document, 2001).

6. Çalişkan, A. and Çevik, U., 'An Efficient Noisy Pixels Detection Model for Ct Images Using Extreme Learning Machines', Tehnički vjesnik, 2018, 25, (3), pp. 679-686.

7. Constant, I. and Sabourdin, N., 'Monitoring Depth of Anesthesia: From Consciousness to Nociception. A Window on Subcortical Brain Activity', Pediatric Anesthesia, 2015, 25, (1), pp. 73-82.

8. Dusan, O.L.M., Rosas, D.A.B., Cagy, M., and Idarraga, R.D.H., 'Nonlinear Analysis of the Electroencephalogram in Depth of Anesthesia', Revista Facultad de Ingeniería, 2015, (75), pp. 45-56.

9. Esmaeili, V., Assareh, A., Shamsollahi, M., Moradi, M., and Arefian, N., 'Estimating the Depth of Anesthesia Using Fuzzy Soft Computation Applied to Eeg', Intelligent Data Analysis, 2008, 12, pp. 393-407.

10. Fu, K., Qu, J., Chai, Y., and Dong, Y., 'Classification of Seizure Based on the Time-Frequency Image of Eeg Signals Using Hht and Svm', Biomedical Signal Processing and Control, 2014, 13, pp. 15-22.

11. Giavarina, D., 'Understanding Bland Altman Analysis', Biochemia medica, 2015, 25, (2), pp. 141-151.

12. Hardman, J.G. and Aitkenhead, A.R., 'Awareness During Anaesthesia', Continuing Education in Anaesthesia, Critical Care & Pain, 2005, 5, (6), pp. 183-186.

13. Hasak, L., Wujtewicz, M., and Owczuk, R., 'Assessment of the Depth of Anaesthesia During Inhalational and Intravenous Induction of General Anaesthesia', Anaesthesiology intensive therapy, 2014, 46, (4), pp. 274-279.

14. Jameson, L.C. and Sloan, T.B., 'Using Eeg to Monitor Anesthesia Drug Effects During Surgery', Journal of clinical monitoring and computing, 2006, 20, (6), pp. 445-472.

15. Jospin, M., Caminal, P., Jensen, E.W., Litvan, H., Vallverdú, M., Struys, M.M., Vereecke, H.E., and Kaplan, D.T., 'Detrended Fluctuation Analysis of Eeg as a Measure of Depth of Anesthesia', Biomedical Engineering, IEEE Transactions on, 2007, 54, (5), pp. 840-846.

16. Lalitha, V. and Eswaran, C., 'Automated Detection of Anesthetic Depth Levels Using Chaotic Features with Artificial Neural Networks', Journal of medical systems, 2007, 31, (6), pp. 445-452.

17. Li, T., Wen, P., and Jayamaha, S., 'Anaesthetic Eeg Signal Denoise Using Improved Nonlocal Mean Methods', Australasian Physical & Engineering Sciences in Medicine, 2014, 37, (2), pp. 431-437.

18. Li, T.-N. and Li, Y., 'Depth of Anaesthesia Monitors and the Latest Algorithms', Asian Pacific journal of tropical medicine, 2014, 7, (6), pp. 429-437.

19. Li, T. and Peng W. Depth of anaesthesia assessment using interval second-order difference plot and permutation entropy techniques. IET Signal Processing 2016, 11, (2), pp.221-227.

20. Liu, Q., Chen, Y.-F., Fan, S.-Z., Abbod, M.F., and Shieh, J.-S., 'Eeg Signals Analysis Using Multiscale Entropy for Depth of Anesthesia Monitoring During Surgery through Artificial Neural Networks', Computational and mathematical methods in medicine, 2015, 2015.

21. Moca, V.V., Scheller, B., Mureşan, R.C., Daunderer, M., and Pipa, G., 'Eeg under Anesthesia—Feature Extraction with Tespar', computer methods and programs in biomedicine, 2009, 95, (3), pp. 191-202.

22. Mousavi, S.M., Adamoğlu, A., Demiralp, T., and Shayesteh, M.G., 'A Wavelet Transform Based Method to Determine Depth of Anesthesia to Prevent Awareness During General Anesthesia', Computational and mathematical methods in medicine, 2014, 2014.

23. Nguyen-Ky, T., Wen, P., and Li, Y., 'Modified Detrended Fluctuation Analysis Method in Depth of Anesthesia Assessment Application', in, Proceedings of the International Conference on Bioinformatics and Computational Biology (BIOCOMP 2008), (CSREA Press, 2008)

24. Nguyen-Ky, T., Wen, P., and Li, Y., 'Theoretical Basis for Identification of Different Anesthetic States Based on Routinely Recorded Eeg During Operation', Computers in biology and medicine, 2009, 39, (1), pp. 40-45.

25. Nguyen-Ky, T., Wen, P., and Li, Y., 'Consciousness and Depth of Anesthesia Assessment Based on Bayesian Analysis of Eeg Signals', Biomedical Engineering, IEEE Transactions on, 2013, 60, (6), pp. 1488-1498.

26. Nguyen-Ky, T., Wen, P., Li, Y., and Gray, R., 'Measuring and Reflecting Depth of Anesthesia Using Wavelet and Power Spectral Density', Information Technology in

11

Biomedicine, IEEE Transactions on, 2011, 15, (4), pp. 630-639.

27. Nicolaou, N., Hourris, S., Alexandrou, P., and Georgiou, J., 'Eeg-Based Automatic Classification of 'Awake'versus 'Anesthetized'state in General Anesthesia Using Granger Causality', PLoS One, 2012, 7, (3), p. e33869.

28. Palendeng, M.E., Wen, P., and Li, Y., 'Real-Time Depth of Anaesthesia Assessment Using Strong Analytical Signal Transform Technique', Australasian Physical & Engineering Sciences in Medicine, 2014, 37, (4), pp. 723-730.

29. Petsiti, A., Tassoudis, V., Vretzakis, G., Zacharoulis, D., Tepetes, K., Ganeli, G., and Karanikolas, M., 'Depth of Anesthesia as a Risk Factor for Perioperative Morbidity', Anesthesiology research and practice, 2015, 2015.

30. Shaker, M.M., 'Eeg Waves Classifier Using Wavelet Transform and Fourier Transform', brain, 2005, 2, p. 3.

31. Shalbaf, R., Behnam, H., and Moghadam, H.J., 'Monitoring Depth of Anesthesia Using Combination of Eeg Measure and Hemodynamic Variables', Cognitive Neurodynamics, 2014, 9, (1), pp. 41-51.

32. Shalbaf, R., Behnam, H., Sleigh, J.W., Steyn-Ross, A., and Voss, L.J., 'Monitoring the Depth of Anesthesia Using Entropy Features and an Artificial Neural Network', Journal of neuroscience methods, 2013, 218, (1), pp. 17-24.

33. Shepherd, J., Jones, J., Frampton, G., Bryant, J., Baxter, L., and Cooper, K., 'Clinical Effectiveness and Cost-Effectiveness of Depth of Anaesthesia Monitoring (E-Entropy, Bispectral Index and Narcotrend): A Systematic Review and Economic Evaluation', Health technology assessment (Winchester, England), 2013, 17, (34), pp. 1-264.

34. Shi, L., Li, X., and Wan, H., 'A Predictive Model of Anesthesia Depth Based on Svm in the Primary Visual Cortex', The open biomedical engineering journal, 2013, 7, p. 71.

35. Spitellie, P.H., Holmes, M.A., and Domino, K.B., 'Awareness During Anesthesia', Anesthesiology Clinics of North America, 2002, 20, (3), pp. 555-570.

36. Staikou, C., Paraskeva, A., Karmaniolou, I., Vezakis, A., and Tsaroucha, A., 'Intravenous Lidocaine Does Not Affect the Anesthetic Depth During Rapid Sequence Induction and Intubation as Assessed by Bispectral Index Monitoring: A Randomized Double Blind Study', Archives of medical science: AMS, 2013, 9, (4), p. 713.

37. Tarasiuk, T., 'Hybrid Wavelet-Fourier Spectrum Analysis', Power Delivery, IEEE Transactions on, 2004, 19, (3), pp. 957-964.

38. Tiren, C., Barr, G., Anderson, R., and Jakobsson, J., 'Depth of Anaesthesia Monitoring: A Clinical Study Comparing Bis and Aai During Heart Surgery: A‐149', European Journal of Anaesthesiology (EJA), 2004, 21, pp. 37-38.

39. Tünsmeyer, J., Hopster, K., and Kästner, S.B., 'Clinical Use of a Multivariate Electroencephalogram (Narcotrend) for Assessment of Anesthetic Depth in Horses During Isoflurane–Xylazine Anesthesia', Frontiers in Veterinary Science, 2016, 3.

39. Tupaika, N., Vallverdu, M., Jospin, M., Jensen, E.W., Struys, M.M., Vereecke, H.E., Voss, A., and Caminal, P., 'Assessment of the Depth of Anesthesia Based on Symbolic Dynamics of the Eeg', in, Engineering in Medicine and Biology Society (EMBC), 2010 Annual International Conference of the IEEE, (IEEE, 2010)

40. Zheng, Y. and Essock, E.A., 'Novel Feature Extraction Method-Wavelet-Fourier Analysis and Its Application to Glaucoma Classification', in, Proceedings of 7th Joint Conference on Information Sciences, (2003)

41. Ziółko, B., Kozłowski, W., Ziółko, M., Samborski, R., Sierra, D., and Gałka, J., 'Hybrid Wavelet-Fourier-Hmm Speaker Recognition', International Journal of Hybrid Information Technology, 2011, 4, (4).

12